pubs.acs.org/acschemicalbiology

Articles

# Inhibitor Mimetic Mutations in the *Pseudomonas aeruginosa* PqsE Enzyme Reveal a Protein–Protein Interaction with the Quorum-Sensing Receptor RhlR That Is Vital for Virulence Factor Production

Isabelle R. Taylor, Jon E. Paczkowski, Philip D. Jeffrey, Brad R. Henke, Chari D. Smith, and Bonnie L. Bassler*

Cite This: *ACS Chem. Biol.* 2021, 16, 740–752

Read Online

ACCESS | Metrics & More | Article Recommendations | Supporting Information

**ABSTRACT:** *Pseudomonas aeruginosa* is an opportunistic human pathogen that causes fatal infections. There exists an urgent need for new antimicrobial agents to combat *P. aeruginosa*. We conducted a screen for molecules that bind the virulence-controlling protein PqsE and characterized hit compounds for inhibition of PqsE enzymatic activity. The binding conformations of two inhibitory molecules, BB391 and BB393, were identified by crystallography, and inhibitor binding was mimicked by the substitution of PqsE residues E182 and S285 with tryptophan. Comparison of the inhibitor-mimetic mutations to the catalytically inactive PqsE D73A protein demonstrated that catalysis is not responsible for the role PqsE plays in driving virulence factor production. Rather, the PqsE E182W protein fails to interact with the quorum-sensing receptor, RhlR, and our results suggest that it is this interaction that is responsible for promoting virulence factor production in *P. aeruginosa*. These findings provide a new route for drug discovery efforts targeting PqsE.

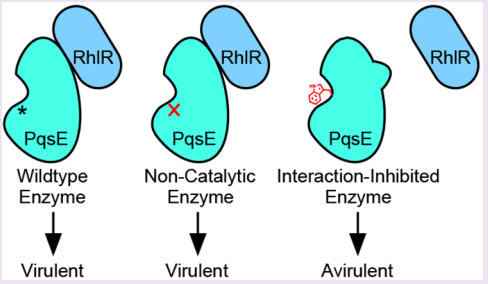


## INTRODUCTION

*Pseudomonas aeruginosa* is a human pathogen that causes life-threatening hospital-acquired infections in immunocompromised patients.[1] *P. aeruginosa* lung infections also occur in cystic fibrosis sufferers,[2] and infections are frequent in severe burn wounds.[3] Traits that drive *P. aeruginosa* clinical pathogenicity include the ability to form biofilms,[4] the production of virulence factors,[5] and antibiotic resistance,[6] which combine to render *P. aeruginosa* infections increasingly unresponsive to treatment.[7,8] Thus, there is an urgent need for new antimicrobial agents targeting this major pathogen.

*P. aeruginosa* virulence factor production and biofilm formation are both under the control of quorum sensing. Quorum sensing is a process of bacterial cell–cell communication that involves the synthesis, release, and detection of small molecule signals, called autoinducers.[9] Multiple quorum-sensing systems exist in *P. aeruginosa*. The most well-studied are the Las and Rhl quorum-sensing systems, which rely on the LasR and RhlR receptors binding the acyl homoserine lactone autoinducers 3-oxo-C12-homoserine lactone (3-oxo-C12-HSL) and C4-homoserine lactone (C4-HSL), respectively.[10−12] Somewhat less understood is the Pqs quorum-sensing system, which employs a class of alkyl quinolone signal molecules, with 2-heptyl-3-hydroxy-4-quinolone (also known as the *Pseudomonas* Quinolone Signal, PQS) as the most comprehensively studied autoinducer of the quinolone class.[13] These three quorum-sensing circuits share overlapping regulons. For instance, Las signaling activates both the Rhl and Pqs systems, and in turn, the Rhl and Pqs systems both control the production of a redox-sensitive toxin called pyocyanin. Pyocyanin is present in the sputum of cystic fibrosis patients with advanced *P. aeruginosa* infections[14,15] and is largely responsible for killing *Caenorhabditis elegans* in a fast-kill model of infection.[5] Pyocyanin also endows *P. aeruginosa* cultures with their characteristic blue-green color. Therefore, the production of pyocyanin is often measured as a convenient readout of *P. aeruginosa* virulence and is considered an output of both Rhl and Pqs quorum sensing.

One particularly intriguing member of the *P. aeruginosa* Pqs quorum-sensing network is *pqsE*, encoding the metallo-*β*-hydrolase enzyme, PqsE. *pqsE* is a member of the *pqsABCDE* operon that encodes all of the necessary components for alkyl quinolone biosynthesis. PqsE has been characterized as an esterase that catalyzes the hydrolysis of 2-amino-benzoyl acetyl CoA to 2-amino-benzoyl acetate (2-ABA), a step in the synthesis of PQS.[16] Curiously, *pqsE* is the only member of the *pqsABCDE* operon that is not absolutely required for PQS production, as other esterases can substitute for this function.[16]

**Received:** January 24, 2021
**Accepted:** March 18, 2021
**Published:** April 1, 2021





https://doi.org/10.1021/acschembio.1c00049
*ACS Chem. Biol.* 2021, 16, 740–752

Nonetheless, deletion of *pqsE* leads to the complete loss of both pyocyanin production in laboratory-grown cultures and infectivity in a mouse model,[17] suggesting a crucial role for PqsE in *P. aeruginosa* pathogenicity. These observations raise the question of whether there exist additional physiologically relevant reactions catalyzed by PqsE and/or whether PqsE carries out functions that do not depend on catalysis. PqsE has been linked to activation of RhlR,[18,19] and indeed, the virulence and biofilm defects of the *P. aeruginosa* Δ*pqsE* mutant closely mirror those of the Δ*rhlR* mutant.[17,20] These findings hint that the relevant function of PqsE in *P. aeruginosa* virulence is associated with the Rhl quorum-sensing system, not the Pqs quorum-sensing system.

The above findings have made PqsE a promising target for the development of *P. aeruginosa* quorum-sensing inhibitors. Unlike RhlR, PqsE can be easily purified, and high-resolution X-ray crystal structures of the protein exist with and without small molecules present in the binding pocket.[21−24] The structures reveal the putative, iron-binding catalytic site, which has been probed by alanine-scanning mutagenesis.[23,25,26] PqsE has measurable *in vitro* enzyme activity with synthetic substrates, making it amenable to high-throughput small molecule screening. Indeed, previous screening efforts have identified molecules that bind PqsE and inhibit its ability to hydrolyze synthetic thioester substrates.[23,27] However, to date, no small molecule PqsE catalytic inhibitor has been discovered that suppresses pyocyanin production in *P. aeruginosa.* Zender *et al.* did report that their identified PqsE enzymatic inhibitors were internalized by *P. aeruginosa* and inhibited PqsE *in vivo*. However, no reduction in pyocyanin production occurred.[23] This finding, combined with data demonstrating that PqsE can sensitize RhlR to C4-HSL in a heterologous *E. coli* assay,[18] again suggest that enzymatic activity might not be the pertinent activity of PqsE with respect to its role in driving virulence factor production.

In this study, we present small molecules discovered in a high-throughput differential scanning fluorimetry screen targeting PqsE, and we demonstrate their use in probing PqsE activities, both enzymatic and nonenzymatic. We solve the X-ray crystal structures of PqsE bound to two enzyme inhibitors obtained through this screen, BB391 and BB393, and we investigate the interactions these inhibitors form in the active site of PqsE. The structural insight afforded by these PqsE−ligand complexes allowed us to develop a structure-guided mutagenesis strategy to determine whether targeting the PqsE active site is an effective means for suppressing *P. aeruginosa* virulence. We uncover a surprising mechanism underpinning PqsE-driven virulence phenotypes involving a direct protein−protein interaction with the RhlR quorum-sensing receptor. Both the chemical tools and the basic biological insight revealed by this work can promote the discovery of new antimicrobial agents targeting PqsE.

## RESULTS

**High-Throughput Differential Scanning Fluorimetry Screen Identifies Small Molecule PqsE Binders.** To discover molecules capable of binding PqsE, without limiting the search to those targeting the putative active site, we conducted a differential scanning fluorimetry (DSF) screen of a 120 000-compound library of drug-like small molecules. This strategy allowed us to identify molecules capable of binding and causing melting temperature ($T_m$) shifts of purified, wildtype (WT) 6xHis-PqsE. For information about the high-throughput screening strategy, refer to the extended methods and see Figures S1 and S2.

Our initial DSF screen was conducted with each compound administered at a concentration of 37 μM. The screen yielded 933 molecules with $|\Delta T_m|$ values of at least 0.75 °C (Figure 1).

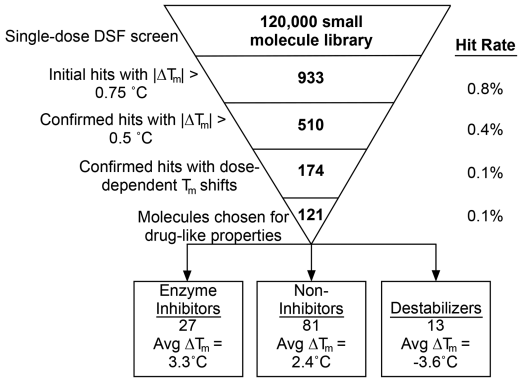


**Figure 1.** Differential scanning fluorimetry screen of a small molecule library containing 120 000 compounds. See text for details.

Retesting of these 933 compounds ($n$ = 4) reduced the hit number to 510 compounds with $|\Delta T_m|$ values of at least 0.5 °C, yielding an initial, confirmed hit rate of 0.4%. To eliminate nonspecific binders, this set of molecules was counter-screened against the purified carbonic anhydrase protein. The remaining compounds (425) were subsequently tested in four-point dose−response DSF assays with PqsE to yield 174 candidate molecules with specific, dose-dependent binding (final hit rate of 0.1%). A total of 121 molecules with good solubility, MW < 500 Da, and low polar surface area were selected for further analysis.

Our first goal was to assess whether the molecules that bound PqsE were also capable of inhibiting its enzymatic activity. To do this, we measured dose-dependent enzyme inhibition by each hit compound using a synthetic ester as the substrate for PqsE. Of the 121 lead molecules, 27 displayed activity as PqsE esterase inhibitors, having $IC_{50}$ values <100 μM. All of the molecules that possessed enzyme inhibitory activity had positive $\Delta T_m$ values. The molecules that bound PqsE but showed no enzyme inhibition up to a test concentration of 100 μM could be divided into two subgroups: those with positive, stabilizing $\Delta T_m$ values and those with negative, destabilizing $\Delta T_m$ values (Figure 1). The molecules possessing destabilizing activity were not investigated further. To date, PqsE enzymatic activity has not been conclusively linked to the role PqsE plays in promoting *P. aeruginosa* virulence phenotypes. Our goal in this work is to characterize the mechanism(s) of action of the PqsE enzyme inhibitor compounds and use what we learn to test whether targeting the active site of this important enzyme can suppress *P. aeruginosa* virulence.

**X-ray Crystallography of Compounds BB391 and BB393 Bound to PqsE Identifies the Residues Involved in Protein−Ligand Interactions in the PqsE Active Site.** We focused on two potent PqsE enzyme inhibitors, BB391 and BB393 (Figure 2a and b, respectively). Both are highly soluble in the buffer used previously to crystallize PqsE, making them suitable for use in structural analyses. PqsE crystals were grown and subsequently soaked with saturating amounts of each compound to obtain crystals of the PqsE-BB391 and PqsE-


https://doi.org/10.1021/acschembio.1c00049
ACS Chem. Biol. 2021, 16, 740−752

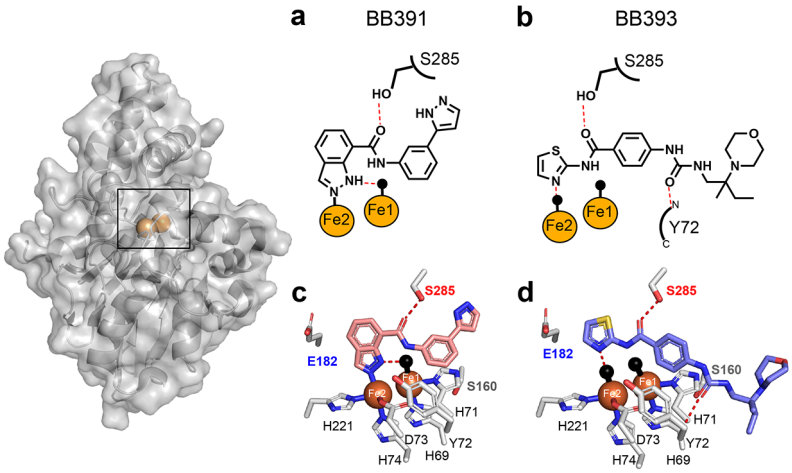


**Figure 2.** Crystal structures of PqsE-BB391 and PqsE-BB393 complexes. Surface and cartoon representations of full-length PqsE shown with iron atoms (orange spheres). In a and b, key interactions for each ligand are depicted with hydrogen bonds shown as red dashed lines and direct bonds are shown as solid lines. Water molecules are depicted as black spheres. In c and d, side chains of select amino acids, including the $^{69}$HXHXDH$^{74}$ motif, that form the PqsE active site are shown in gray with nitrogen atoms in blue and oxygen atoms in red. BB391 and BB393 nitrogen and oxygen atoms use the same coloring scheme. Carbon atoms are shown in pink for BB391 and light blue for BB393, and the sulfur atom in BB393 is in yellow. Hydrogen bonds, water molecules, and iron atoms appear as in a and b.

BB393 complexes. The PqsE active site contains two iron atoms coordinated by a total of five histidine and two aspartate side chains, with the irons bridged by D178 and a water molecule.[25] Both irons are hexacoordinate with a water molecule or ligand atom occupying an axial position. The active site is accessible to solvent at one end and essentially blocked by the E182 side chain at the other. The binding pocket is relatively narrow in one direction, orienting planar ligands edge-on to the iron atoms, and the central portion is lined primarily with hydrophobic residues (L193, F195, F276, L277, L281, H282, M286). The cocrystal structures demonstrate that both BB391 and BB393, as expected, bind in the reported PqsE active site (Figure 2), with no evidence of the protein undergoing any conformational change upon ligand binding. In the case of BB391, N2 of the indazole ring coordinates directly with the Fe2 ion (Fe−N bond 2.11 Å), and N1 participates in hydrogen bonding with the axial water ligand of Fe1 at the solvent-exposed end of the pocket (Figure 2a,c). Regarding BB393, no direct coordination of the Fe ions is observed, and the nitrogen atom of the thiazole group forms a short hydrogen bond (2.27 Å) with the axial water ligand of Fe2 (Figure 2b,d). Also, in the PqsE-BB393 structure, a water molecule occupies the location of the N2 atom of BB391 in the PqsE-BB391 structure, as the amidothiazole of BB393 is too small to make direct interactions with Fe2. Both BB391 and BB393 possess amide bonds, and both crystal structures reveal that the carbonyl oxygens of the amides form a hydrogen bond with the side-chain hydroxyl group of S285 (2.36 Å with BB391 and 2.35 Å with BB393). This hydrogen bond is formed by both BB391 and BB393 despite the direction of the amide bond being reversed in their respective binding poses. BB393 makes one additional polar contact through the O2 of the urea moiety with the backbone amide of the tyrosine at position 72 (Y72), an interaction that BB391 lacks. Thus, although BB391 and BB393 possess different core scaffolds, they both display similar interactions with PqsE in the interior iron-containing region of the ligand binding pocket, suggesting conformational restrictions in this portion of the binding site as a consequence of hydrogen bonding from S285 to the ligand amide moieties and the overall flattened shape of the binding pocket.

Compared to previously reported PqsE structures, the structure of the PqsE-BB393 complex highlights the ability of a small molecule to make weak secondary interactions in a shallow, hydrophobic region at the solvent-exposed periphery of the ligand binding pocket. The BB393 C10 chiral center is situated in a hydrophobic groove formed between the face of the $\alpha$-helix consisting of PqsE residues S104−L116 and the backbone of the $^{69}$HXHXDH$^{74}$ motif (Figure 2c,d) characteristic of this class of hydrolase enzymes. The orientation of C10 in this groove additionally forces the morpholine ring of BB393 out of the pocket and into the solvent. This structure suggests that additional, nonpolar moieties could be accommodated on compounds that are situated at the solvent-facing region peripheral to the binding pocket, encouraging further lead optimization to introduce substituents that bind in this hydrophobic groove. Moreover, the PqsE-BB393 structure shows that the (*R*)-enantiomer of BB393 is present, even though racemic BB393 was used for soaking. The hydrogen bond between the main-chain of Y72 and the urea moiety of BB393 (2.81 Å) likely influences the stereoselectivity at this site by reducing the conformational flexibility of this region of BB393. This result suggests a stereoselective interaction between BB393 and PqsE that could be exploited to potentially improve potency.

**Fluorescent Probe Design and Competitive Binding Assays.** The PqsE−BB391 structure showed that there is space at the solvent-facing portion of the binding pocket that could accommodate derivatization at the *para* position on the BB391 phenyl group. Thus, we generated a fluorescent probe based on the BB391 core scaffold to enable competitive binding assays for mechanistic studies of PqsE inhibitors. The fluorescent probe, BB562 (Figure 3a), did indeed bind to purified WT PqsE as shown using fluorescence polarization, with an apparent binding constant ($K_{app}$) in the midnanomolar range (Figure 3b). This result demonstrates that BB562 can be used as a tool to assess whether small molecules have sufficient affinity to compete for binding in the active site.


https://doi.org/10.1021/acschembio.1c00049
ACS Chem. Biol. 2021, 16, 740−752

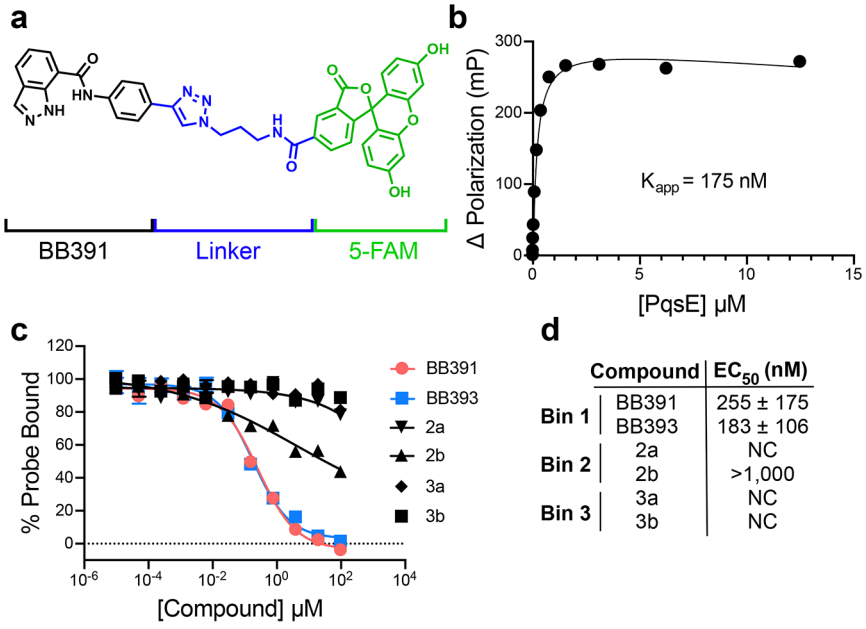


**Figure 3.** Compounds that bind in the PqsE active site compete with a fluorescent BB391-based probe. (a) Structure of a 5-FAM-containing fluorescent probe called BB562. The BB391 portion is in black, the linker is in blue, and the 5-FAM moiety is in green. (b) Binding curve for WT PqsE to BB562. $K_{app}$ was determined from two independent experiments performed in triplicate. (c) Competition of select screening hit compounds from the DSF screen, including BB391 and BB393, against BB562 for binding to PqsE. The fluorescence polarization value for PqsE-BB562 in the absence of a competitor is defined as 100% probe bound. The dotted line at 0 represents the level of background fluorescence polarization which was subtracted from the results depicted here. (d) Calculated $EC_{50}$ values for compounds in c, determined from two independent experiments performed in triplicate. Error bars are present in all cases and represent standard deviations. Some error bars are smaller than the symbols.

The fluorescent BB562 probe was used in competitive binding assays to determine whether hit molecules identified from the primary DSF screen were capable of competing for binding in the PqsE active site. Consistent with their binding poses in the crystal structures, both BB391 and BB393 competed with BB562 for binding WT PqsE with $EC_{50}$ values of 255 nM and 183 nM, respectively (Figure 3c,d Bin 1). Additionally, we tested molecules from each of the other categories of screening hits: the noninhibiting binders (Bin 2) and the destabilizers (Bin 3). Notably, these screening hits were only weakly competitive at best (compound **2b**) or were incapable of competing with the probe (compounds **2a**, **3a**, and **3b**). Curiously, the destabilizing compounds (**3a** and **3b**) do not appear to affect the ability of PqsE to bind the BB562 probe. In the original screen, the negative $T_m$ shifts induced by these compounds reduced the observed $T_m$ from ∼68 °C to roughly 50−60 °C. One possible explanation for the results in Figure 3 is that because the competitive binding assay is performed at RT, under this condition, PqsE is not sufficiently destabilized by compounds **3a** and **3b** to affect its ability to bind BB562 in the active site.

**PqsE Residues E182 and S285 Are Required for Inhibition by BB391 but Not BB393.** Guided by the crystal structures of PqsE bound to BB391 and BB393, we next investigated the amino acids responsible for forming the crucial protein−ligand interactions. We focused on two residues: S285 and E182 (Figure 2c,d). Our rationale is as follows: the hydroxyl group of S285 participates in hydrogen bonding with the amide groups of both BB391 and BB393, suggesting that S285 can mediate an important interaction between the protein and each ligand. E182 has previously been suggested to act as a gating residue for the most interior region of the PqsE binding pocket. Specifically, PqsE E182A possesses increased hydrolytic activity with a synthetic phosphodiester substrate, bis(*p*-nitrophenyl) phosphate, due to elimination of a steric clash when the glutamic acid residue is replaced with the shorter, uncharged alanine residue (ref 25 and verified in Figure S3).

To determine whether the presence of the PqsE E182 and S285 residues is necessary for binding and/or inhibition by BB391 and BB393, we constructed PqsE E182A and PqsE S285A and purified the two mutant proteins. As a control, we also generated and purified PqsE S160A, as the crystal structures show that residue S160 is not involved in binding either molecule (Figure 2c,d). All proteins purified in this study exhibited >95% purity as judged by SDS-PAGE analysis (Figure S4). We also assayed a previously reported PqsE-inhibiting fragment molecule, 2-(pyridin-3′-yl) benzoic acid (called C1).[23] The X-ray crystal structure of C1 bound to PqsE indicates that unlike BB391 and BB393, C1 does not interact with S285, nor does it abut E182. Consistent with this observation, the $\Delta T_m$ values for C1 binding to PqsE E182A, PqsE S285A, and PqsE S160A were similar to those for C1 binding to WT PqsE (WT $\Delta T_m$ = 8.7 °C and $\Delta T_m$ = 10 °C, 8.5 °C, and 12.1 °C for PqsE E182A, PqsE S285A, and PqsE S160A, respectively, Figure 4a−d). We note that the PqsE S160A control protein has a considerably lower intrinsic $T_m$ than WT PqsE in the absence of a small molecule (61.6 °C vs 67.2 °C, respectively) possibly explaining the increased $\Delta T_m$ observed for C1 binding to PqsE S160A. The PqsE S160A protein behaved like WT PqsE with respect to stabilization by our molecules, as both BB391 and BB393 induced shifts in the PqsE S160A $T_m$ similar to that for WT PqsE ($\Delta T_m$ WT PqsE = 3.4 and 7.2 °C, and $\Delta T_m$ PqsE S160A = 5.0 and 8.5 °C for


https://doi.org/10.1021/acschembio.1c00049
ACS Chem. Biol. 2021, 16, 740−752

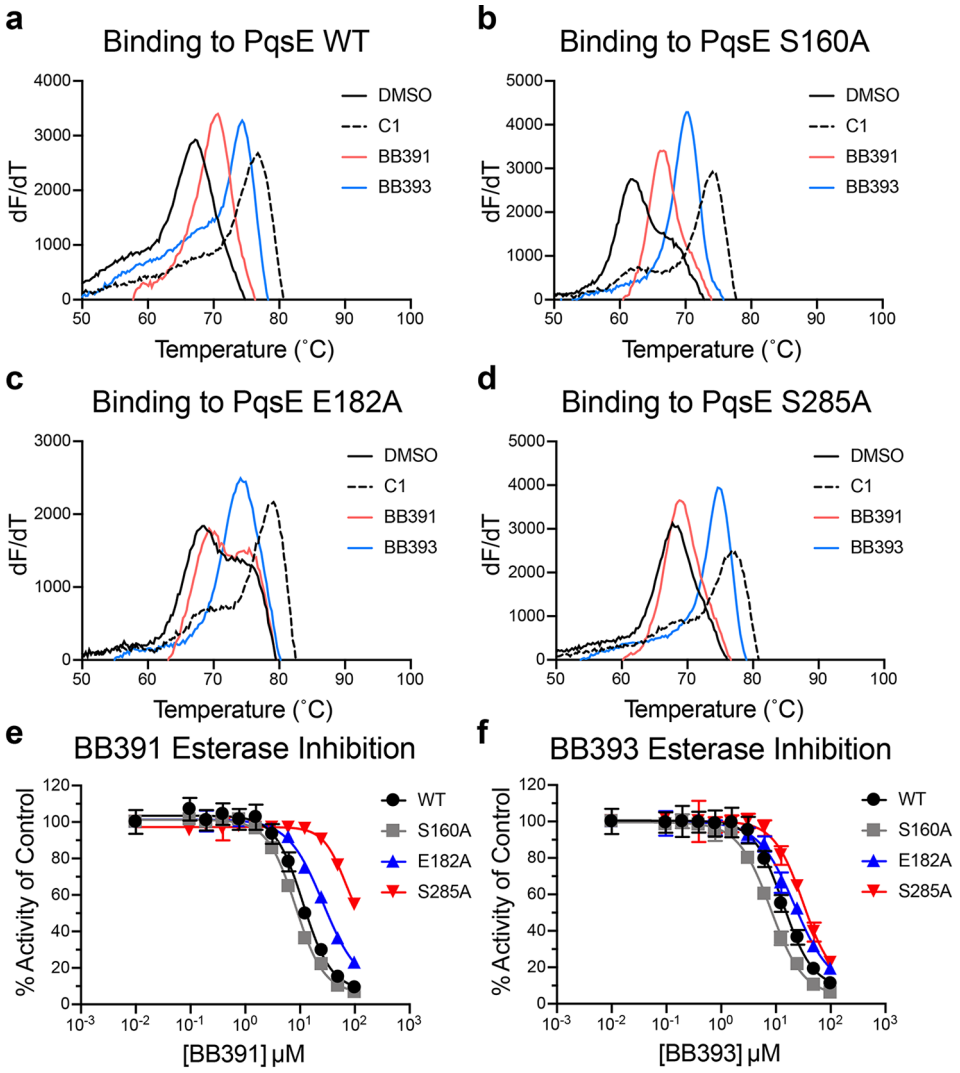


**Figure 4.** PqsE E182 and PqsE S285 are required for binding to BB391 but not BB393. First-derivative plots (dF/dT is defined as the change in SYPRO Orange fluorescence divided by the change in temperature) of melting curves for (a) WT PqsE, (b) PqsE S160A, (c) PqsE E182A, and (d) PqsE S285A in the presence of 5% DMSO (black solid lines), 100 $\mu$M C1 (black dashed lines), 100 $\mu$M BB391 (pink lines), and 100 $\mu$M BB393 (blue lines). In all cases, PqsE protein was at 5 $\mu$M. The peak of each curve is defined as the $T_m$. (e) BB391 and (f) BB393 esterase inhibition dose−response curves for the designated PqsE proteins. PqsE proteins and MU-butyrate were used at concentrations of 200 nM and 2 $\mu$M, respectively. Two independent experiments were performed in triplicate. Error bars represent standard deviations.

BB391 and BB393, respectively; Figure 4a,b). BB391, by contrast, lost the ability to shift the $T_m$ of PqsE E182A and PqsE S285A, suggesting that BB391 has reduced affinity for these PqsE variants (Figure 4c,d). Surprisingly, neither the PqsE E182A nor the S285A mutations altered the stabilizing effect of BB393 (Figure 4c,d). We reason that, unlike C1 and BB391, BB393 makes more extensive interactions in the binding pocket of PqsE, and therefore its affinity for PqsE is not perturbed by the loss of any single interaction with any single amino acid.

We investigated whether the amino acid substitutions we introduced into PqsE affect its esterase activity and whether the changes impinge on the abilities of BB391 and BB393 to function as PqsE inhibitors. In the absence of inhibitors, all three mutant proteins (PqsE E182A, PqsE S285A, and the control protein PqsE S160A) displayed 69−109% of WT PqsE esterase activity against a synthetic substrate 4-methylumbelliferyl butyrate (MU-butyrate;[28,29] Figure S5). Thus, none of these three residues is required for catalysis. However, BB391 exhibited significantly decreased potency against PqsE E182A compared to WT PqsE and PqsE S160A. An accurate assessment of the $IC_{50}$ of BB391 for PqsE S285A could not be determined due to its incomplete inhibition profile, but the projected $IC_{50}$ was at least a log unit higher than that observed for WT PqsE (Figure 4e). Thus, PqsE residues E182 and S285 are important for BB391 to function as an inhibitor. Strikingly, the PqsE E182A and S285A substitutions had almost no effect on the inhibitory potency of BB393 (Figure 4f). The interpretation for PqsE S285 and BB391 is straightforward from the crystal structure: S285 hydrogen bonds with BB391, and substitution with an alanine eliminates this interaction. Regarding the ability of BB393 to inhibit PqsE S285A, we hypothesize that due to the larger size of BB393 relative to BB391, and its more extensive interactions with PqsE residues, individual amino acid substitutions in PqsE are not capable of perturbing BB393 binding. The results with PqsE E182A are less obvious because of the lack of hydrogen bonding with either of the two inhibitors and in light of a previous study


https://doi.org/10.1021/acschembio.1c00049
ACS Chem. Biol. 2021, 16, 740−752

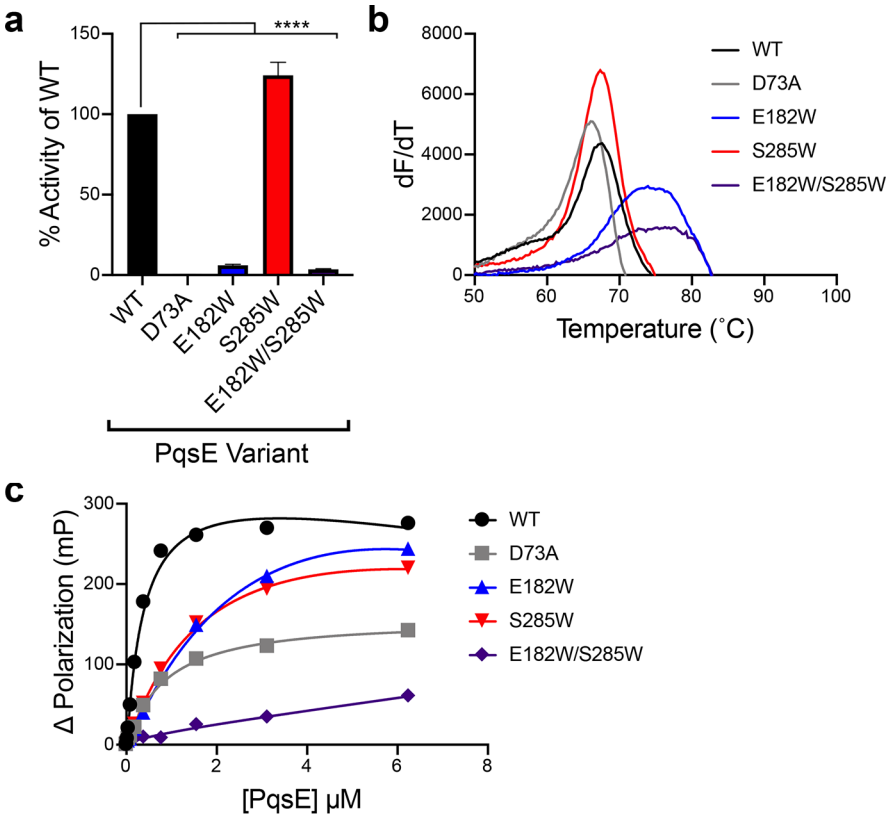


**Figure 5.** PqsE E182W and PqsE E182W/S285W mimic the effect of PqsE inhibition *in vitro*. (a) Hydrolysis of 4-methyl-umbelliferyl butyrate by the designated PqsE proteins. Values are represented as % of the WT PqsE activity. Two independent experiments were performed in triplicate. ****$P < 0.0001$ in one-way ANOVA compared to WT. (b) First derivative plots (dF/dT is defined as the change in SYPRO Orange fluorescence divided by the change in temperature) of melting curves for the designated PqsE proteins. The peak of each curve is defined as the $T_m$. (c) Binding of the designated PqsE proteins to BB562. Binding curves were generated from two independent experiments performed in triplicate. Error bars are present in all cases and represent standard deviations. Some error bars are smaller than the symbols.

showing an increased capacity for PqsE E182A to interact with particular artificial substrates.[25] We hypothesize that PqsE residue E182 plays a role in stabilizing the interior region of the binding pocket, and mutation to alanine changes the context of inhibitor binding in this region. The BB391 indazole ring appears to bind more deeply in the PqsE active site pocket than does the thiazole ring of BB393, possibly explaining why the E182A mutation affects inhibition by BB391 more severely than it affects inhibition by BB393.

**Structure-Guided Introduction of Tryptophan Residues to Produce PqsE Proteins That Mimic the Inhibited State.** To gain deeper mechanistic insight into whether PqsE enzyme inhibitors have the potential to suppress virulence in *P. aeruginosa*, we used a structure-guided approach to design inhibitor-binding mimetic mutations in the PqsE enzyme active site. On the basis of the crystal structures of BB391 and BB393 bound to PqsE and the above results of our analyses with the purified proteins containing alanine substitutions, we engineered and purified PqsE E182W, PqsE S285W, and PqsE E182W/S285W rationalizing that these alterations could simulate the binding of a space-filling inhibitory ligand. As a reminder, neither the E182 nor the S285 residue is required for catalysis (Figure S5), making them appropriate residues for substitution with the bulky tryptophan residue without issues arising from loss of catalytic activity that would confound our studies. Because PqsE is a metallo-enzyme and contains a conserved HXHXDH motif, we reasoned that the aspartic acid, D73, in this motif is the key residue involved in the PqsE catalytic mechanism, consistent with validated mechanisms for other metallo-hydrolases.[30] Thus, we also constructed and purified the PqsE D73A variant (Figure S4) to compare the behavior of a catalytically inactive PqsE protein to the potential inhibitor mimic variants, as we do not necessarily expect those different PqsE states to exhibit identical activities. In agreement with our predictions regarding the identities of catalytic residues in the active site, PqsE D73A had undetectable activity in the *in vitro* enzyme assay for hydrolysis of MU-butyrate (Figure 5a). PqsE E182W and PqsE E182W/S285W each displayed less than 10% of the catalytic activity of WT PqsE (Figure 5a). On the other hand, the PqsE S285W mutant displayed modestly increased hydrolytic activity (124%) compared to WT PqsE. Thus, PqsE D73A is catalytically inactive, PqsE E182W and PqsE E182W/S285W behave as if they have an inhibitor bound, and PqsE S285W behaves like WT PqsE with respect to enzyme activity.

To further compare the characteristics of the catalytically inactive mutant to the putative inhibitor-bound PqsE mimetics, we determined their melting temperatures using DSF. PqsE variants containing the E182W substitution had higher intrinsic $T_m$ values than WT PqsE, showing that insertion of a tryptophan residue at this location stabilizes the protein (Figure 5b). Specifically, the $T_m$ shifts for PqsE E182W and PqsE E182W/S285W were similar to the $\Delta T_m$ observed following the addition of high concentrations of BB391 or BB393 to WT PqsE ($\Delta T_m \approx 10$ °C), suggesting that introduction of a tryptophan residue at position 182 mimics


https://doi.org/10.1021/acschembio.1c00049
ACS Chem. Biol. 2021, 16, 740−752

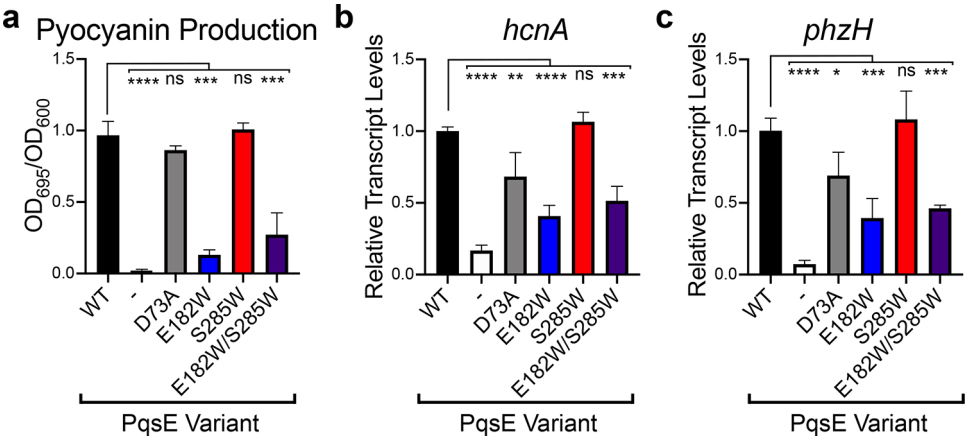


**Figure 6.** Mimicking PqsE enzyme inhibition in *P. aeruginosa* decreases pyocyanin production. (a) Shown is pyocyanin production by the Δ*pqsE P. aeruginosa* strain carrying the designated *pqsE* alleles on the pUCP18 plasmid. The "-" symbol designates the strain carrying the empty pUCP18 vector. The $OD_{695}$ values of cell-free culture fluids were normalized to the $OD_{600}$ of the cultures. The % pyocyanin production reported is relative to that of the strain carrying WT PqsE. The results shown are the average of two biological replicates. Error bars represent standard deviations. (b) Relative abundance of the *hcnA* transcript in the designated strains compared to WT, determined by qRT-PCR. (c) As in b for *phzH*. Results shown are the average of three biological replicates performed in quadruplicate. ns = not significant, ****$P < 0.0001$, ***$P < 0.0005$, **$P < 0.005$, *$P < 0.05$ in one-way ANOVA compared to WT.

the effect of a bound inhibitor. The PqsE E182W substitution clearly provides the stabilizing interactions observed in the PqsE E182W/S285W protein since PqsE S285W had the same $T_m$ as WT PqsE (Figure 5b). Moreover, this result shows that the single S285W substitution in PqsE does not produce a phenotype mimicking the inhibitor-bound state. Each of the PqsE single tryptophan variants exhibited a ∼5−10-fold reduction in affinity for the BB562 fluorescent probe ($K_{app}$ = 5.1 μM and 2.2 μM for PqsE E182W and PqsE S285W, respectively, vs 0.4 μM for WT PqsE), and the PqsE E182W/S285W double mutant protein failed to bind BB562 (Figure 5c). Collectively, these *in vitro* results show that introduction of a tryptophan in place of the E182 residue in the PqsE active site produces effects similar to those that occur following treatment with the BB391 or BB393 inhibitors, and the PqsE E182W alteration can be combined with the S285W alteration to nearly completely block small molecule binding in the active site. By contrast, the PqsE D73A protein exhibited a similar $T_m$ to that of WT PqsE (Figure 5b) and bound the BB562 probe with a similar affinity as WT PqsE ($K_{app}$ = 0.9 μM for PqsE D73A; Figure 5c), suggesting that the effect of tryptophan insertion at position 182 is related to blocking substrate access to the active site and not to affecting the catalytic mechanism. We note that although the $K_{app}$ for PqsE D73A is relatively unchanged compared to WT PqsE, the maximum change in fluorescence polarization observed for this mutant was lower than that for WT PqsE. We interpret this result to indicate a difference in the conformation of the BB562-bound mutant protein relative to WT PqsE bound to BB562, rather than altered affinity for the probe. It is unlikely that mutation of PqsE E182 or S285 to tryptophan perfectly recapitulates the effects of BB391 or BB393 binding in the active site. Nonetheless, these mutants provide powerful tools to explore the consequences of filling the PqsE active site. For simplicity, in the remainder of this work, we refer to these PqsE E182W and PqsE S285W mutants as "inhibitor mimetics."

**Mimicking Inhibitor Binding to PqsE Suppresses *P. aeruginosa* Virulence Traits *in Vivo*.** Our results show that BB391 and BB393 represent promising starting points for *in vivo* inhibitors of PqsE enzymatic activity. However, when administered to cultures of *P. aeruginosa* PA14, neither molecule caused any decrease in pyocyanin production (Figure S6a). Likewise, neither molecule drove altered transcription of the virulence associated *hcnA* (hydrogen cyanide production) and *phzH* (phenazine biosynthesis) genes, both of which are known to be regulated by PqsE (Figure S6b,c, respectively).[31] Two possibilities could explain this result: first, the molecules are inactive *in vivo* due to low cell permeability, metabolism, and/or efflux, or second, targeting the active site of PqsE with small molecule inhibitors does not affect the *P. aeruginosa* pyocyanin virulence trait. The latter explanation has been proposed to underpin the finding that, when administered to *P. aeruginosa* PAO1, the inhibitor C1 did not affect pyocyanin production.[23] To distinguish between these possibilities for our inhibitors, we introduced WT PqsE and the inhibitor bound mimetic PqsE proteins into Δ*pqsE P. aeruginosa* PA14 and assessed whether PqsE-driven virulence phenotypes were altered. We also examined the effects of the catalytically inactive PqsE D73A variant. In all cases, the PqsE alleles were fused to C-terminal His tags. Western blot analysis showed that the different PqsE proteins were soluble and produced at similar levels in Δ*pqsE P. aeruginosa* PA14 (Figure S7).

Unlike WT *P. aeruginosa* PA14, the Δ*pqsE* strain carrying the empty pUCP18 vector produced almost no pyocyanin (2% of WT; Figure 6a). The strain carrying the catalytically inactive PqsE D73A variant produced pyocyanin levels similar to the WT strain. While this result supports the interpretation of Zender et al.,[23] that PqsE plays a nonenzymatic regulatory role in virulence, it is surprising in light of other mutagenic analyses showing that amino acid substitutions predicted to affect catalytic activity also affected pyocyanin production *in vivo*.[26] The Δ*pqsE P. aeruginosa* PA14 strains carrying PqsE alleles with the E182W substitution displayed striking impairments in pyocyanin production (compared to WT PqsE, PqsE E182W = 14% and PqsE E182W/S285W = 27% activity; Figure 6a). Surprisingly, the *P. aeruginosa* strain carrying the PqsE E182W/S285W mutant protein produced more pyocyanin than did the strain carrying PqsE E182W. We return to this point below. Consistent with our *in vitro* results, the strain harboring the PqsE S285W variant showed no change in


https://doi.org/10.1021/acschembio.1c00049
ACS Chem. Biol. 2021, 16, 740−752

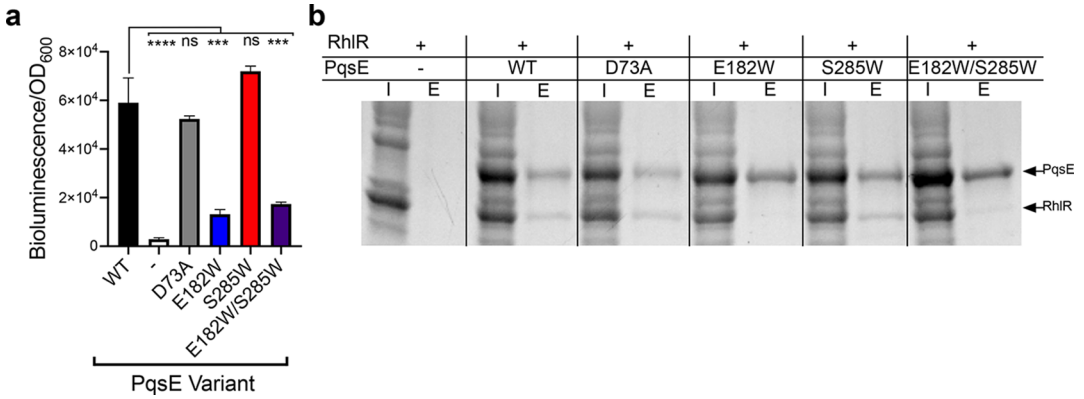


**Figure 7.** PqsE interacts with RhlR and increases RhlR sensitivity to C4-HSL. (a) Bioluminescence output from *E. coli* carrying *rhlR*, *rhlA-luxCDABE*, and the designated *pqsE* alleles on the pACYC184 plasmid in response to 200 nM C4-HSL, normalized to the $OD_{600}$ of the cultures. The "-" symbol designates the strain carrying the empty pACYC184 vector. The results shown are the average of two biological replicates performed in duplicate. Error bars represent standard deviations. ns = not significant, ****$P < 0.0001$, ***$P < 0.0005$ in one-way ANOVA compared to WT. (b) SDS-PAGE analysis of input (I) and elution (E) samples from PqsE−RhlR pull-down assays. 6xHis-PqsE was immobilized on Ni resin and exposed to lysate containing RhlR. On the gel, 6xHis-PqsE appears as a ∼34 kDa band and RhlR-mBTL as a ∼28 kDa band.

pyocyanin phenotype compared to the strain harboring WT PqsE. Together, the results with the catalytically inactive PqsE D73A and the PqsE E182W and E182W/S285W variants that mimic the inhibitor bound state suggest there could be a nonenzymatic activity of PqsE that is primarily responsible for the virulence phenotypes in *P. aeruginosa*. Underscoring the relevance of the pyocyanin production profiles, analogous results were obtained for transcription of the virulence genes *hcnA* and *phzH* in *P. aeruginosa* carrying the different PqsE variants (Figure 6b,c, respectively).

**PqsE Sensitizes RhlR to C4-HSL through a Protein−Protein Interaction and Inhibitor Mimetic Mutations Disrupt This Activity.** We considered the possibility that the putative nonenzymatic role for PqsE in promoting *P. aeruginosa* PA14 virulence could concern the connection of PqsE to the Rhl quorum-sensing system. To explore this hypothesis, we took advantage of the previous finding that coexpression of *pqsE* together with *rhlR* in recombinant *Escherichia coli* sensitizes RhlR to exogenous addition of its native autoinducer, C4-HSL, by 2−20-fold.[18,23] Because this effect occurs in a heterologous system, it enables study of the synergistic PqsE−RhlR activity in isolation. We hypothesize that it is this coupled PqsE−RhlR activity, not PqsE catalytic activity, that is key for PqsE to promote virulence. If so, our PqsE inhibited mimetics could display decreased abilities to sensitize RhlR to C4-HSL in this assay. To test this possibility, we constructed an *E. coli* strain harboring three plasmids: a plasmid with *rhlR* expressed under an inducible $P_{BAD}$ promoter, a plasmid with a P*rhlA-luxCDABE* bioluminescent reporter of RhlR transcriptional activity, and a pACYC184 plasmid that drives constitutive expression of WT *pqsE*, *pqsE* D73A, *pqsE* E182W, *pqsE* S285W, or *pqsE* E182W/S285W. Compared to the empty pACYC184 vector control, introduction of WT PqsE enhanced the RhlR response to 200 nM C4-HSL by ∼20-fold (Figure 7a). Introduction of PqsE D73A drove an equivalent augmentation of the RhlR response (Figure 7a), showing that the PqsE-driven enhancement of RhlR activity in this system does not require PqsE catalytic activity. Likewise, PqsE S285W was fully capable of sensitizing RhlR to C4-HSL. However, both PqsE E182W and PqsE E182W/S285W were severely defective in sensitizing RhlR to C4-HSL (23% and 30% of WT activity, respectively). Thus, the ability of PqsE to stimulate RhlR activity in this assay tracks with the ability of PqsE to drive pyocyanin production *in vivo*.

To test whether PqsE and RhlR form a complex, we purified each of our PqsE proteins containing N-terminal 6xHis tags and immobilized them on Ni resin. We exposed the immobilized PqsE proteins to lysate containing RhlR. As previously reported, addition of the artificial RhlR ligand called *meta*-bromo-thiolactone (mBTL) to *E. coli* cultures is required to isolate soluble, folded RhlR.[32] Hence, we refer to the RhlR purified in this study as RhlR-mBTL. We next eluted the proteins and used SDS-PAGE to assess whether RhlR-mBTL had bound to WT PqsE and any of the variants. Strikingly, WT PqsE, PqsE D73A, and PqsE S285W formed complexes with RhlR-mBTL. However, almost no RhlR-mBTL copurified with PqsE E182W or PqsE E182W/S285W (Figure 7b). We interpret this result to mean that PqsE and RhlR physically interact, and this interaction is related to the activation of pyocyanin production *in vivo*. Our evidence also suggests that PqsE catalytic activity is dispensable for this function. It is curious that the PqsE E182W mutation strongly impairs the PqsE−RhlR-mBTL interaction given that the E182 residue is buried in the core of the protein (Figure 2). This finding suggests that this key residue does not itself interact with RhlR. Rather, we propose that there is an allosteric connection between the active site of PqsE and the RhlR-interaction site.

Although the PqsE E182W and S285W mutations were designed to mimic the binding of small molecule inhibitors in the active site, neither BB391 nor BB393 suppressed the interaction between PqsE and RhlR (Figure S8). This result implies that the inhibitor mimic mutations do not fully replicate the effects of BB391 and BB393 binding. Perhaps this finding should not be surprising given that BB391 and BB393 binding to PqsE did not drive large-scale conformational changes (Figure 2). Our current efforts are focused on structural characterization of PqsE E182W and linking conformational changes in the mutant protein to the RhlR interaction interface.

As mentioned in the preceding section, the *P. aeruginosa* PqsE E182W/S285W strain produced more pyocyanin than the *P. aeruginosa* PqsE E182W strain (Figure 6). The pulldown interaction assay in Figure 7 mirrors this finding, showing that


https://doi.org/10.1021/acschembio.1c00049
ACS Chem. Biol. 2021, 16, 740−752

the PqsE E182W/S285W mutant exhibited more interaction with RhlR-mBTL than did the PqsE E182W mutant. We do not yet understand the molecular basis for these parallel results, but it appears that alteration of PqsE S285 to tryptophan, when in the context of the PqsE E182W mutation, somewhat abrogates the defect caused by the change of E182 to tryptophan.

## DISCUSSION

*P. aeruginosa* remains a significant human health burden with tragic outcomes for immunocompromised individuals who acquire infections. *P aeruginosa* is a member of the ESKAPE class of highly resistant pathogens, making development of antimicrobials that are effective in treating *P. aeruginosa* infections a high-priority pursuit.[7,24,33] In this study, we contribute to this effort by identifying small molecules targeting the *P. aeruginosa* virulence-controlling protein, PqsE. Successful modulation of PqsE could deliver a new class of antimicrobial agents that function by disrupting quorum-sensing-mediated cell−cell communication. Our approach exploited differential scanning fluorimetry to identify high-affinity PqsE binders, a strategy that was unbiased as to binding site or mechanism of action. We classified hit molecules as inhibitory or noninhibitory in a secondary assay quantifying PqsE enzymatic activity. Our follow-up characterization was focused on inhibitory compounds with chemical properties most amenable to further synthetic diversification. However, we note that the screen yielded an additional ∼80 confirmed binders that did not affect PqsE enzyme activity, as well as molecules that destabilized PqsE. All of these uncharacterized screening hits present opportunities for future analyses, mechanistic investigation, and potential therapeutic development. We highlight the compounds that destabilized PqsE as destabilization of PqsE could represent an especially attractive mechanism for impairing PqsE function to control virulence *in vivo*.

Based on their high affinity binding and desirable chemical features, hit molecules BB391 and BB393 were prioritized as amenable to structural analysis to identify their binding conformations in the active site of PqsE. The crystal structures presented here of the PqsE-BB391 and PqsE-BB393 complexes represent the first inhibitor-bound crystal structures of PqsE in which the bound inhibitor is not a small nonoptimized fragment but rather, a larger, drug-like ligand. These structures provide valuable information that can be used to inform future medicinal chemistry campaigns against PqsE. Moreover, the structures enabled analyses of the roles key residues play in the PqsE active site. Indeed, the structures guided the design of amino acid substitutions to generate PqsE variants that mimic the enzyme in an inhibitor-bound state. Tryptophan scanning mutagenesis has historically been used to enable structural characterization of transmembrane channels and other metastable proteins.[34−37] However, the strategy of introducing tryptophan substitutions to mimic ligand binding as used here is underexplored and presents a potentially exciting route to pursue for validation of promising drug targets and investigation of inhibitor mechanisms of action for soluble cytoplasmic proteins.

In the realm of inhibitor target validation, *P. aeruginosa* presents a particularly daunting problem, as this pathogen is remarkably impermeable to small molecule reagents, possesses multiple drug efflux pumps, and voraciously metabolizes compounds of varied structures.[38,39] Thus, it has often been impossible to accurately assess whether compounds with interesting *in vitro* activities are nonfunctional *in vivo* in *P. aeruginosa* or, alternatively, whether such compounds simply do not reach the cytoplasmic target for the reasons mentioned above. Our strategy of generating PqsE inhibitor mimetics enabled us to garner evidence suggesting there is indeed merit to the approach of inhibiting PqsE to suppress *P. aeruginosa* virulence. Moreover, our data confirm that, although the mechanism may not involve inhibition of catalytic activity, small molecule binding in the PqsE active site may suppress *in vivo* virulence traits. The work here also provides tools for new screens to identify molecules that affect the PqsE−RhlR interaction. For instance, the heterologous reporter system used in this study could be easily customized to enable high-throughput small molecule screening, potentially enabling identification of inhibitors of the PqsE−RhlR coupled activity that can subsequently be tested in *P. aeruginosa*.

Our data suggest that while PqsE catalytic activity (as judged by the catalytically inactive PqsE D73A variant) is not involved in regulating virulence factor production, mimicking the PqsE inhibited state (as judged by the PqsE E182W and PqsE E182W/S285W variants) does indeed confer a profound defect in a *P. aeruginosa* virulence phenotype: pyocyanin production. The question of whether targeting the PqsE active site has the potential to decrease *P. aeruginosa* virulence has been posed previously.[23] The conundrum was that small molecules that inhibited PqsE *in vitro* were unable to suppress pyocyanin production *in vivo*. These results were interpreted to mean that PqsE has a nonenzymatic regulatory role in controlling *P. aeruginosa* virulence factor production. Our findings using our series of PqsE inhibitor mimetic mutants support this supposition. Furthermore, the *in vitro* physical interaction of each of our PqsE mutants with RhlR correlates with the corresponding *in vivo* pyocyanin production level that occurs when each mutant protein is present in *P. aeruginosa* PA14. We propose that complex formation enables PqsE to sensitize RhlR to its cognate autoinducer, C4-HSL, which upregulates RhlR-controlled virulence phenotypes. We caution that this protein−protein interaction has yet to be confirmed in *P. aeruginosa*, a focus of our ongoing work. Nonetheless, our data show that the PqsE variants that are incapable of interacting with RhlR *in vitro* closely mirror their inabilities to promote pyocyanin production and to drive transcription of *hcnA* and *phzH* in *P. aeruginosa*. These results support our interpretation that it is this PqsE−RhlR physical interaction, and not PqsE enzymatic activity, that is relevant to virulence. Moreover, we posit that targeting the PqsE−RhlR interaction should be prioritized in the pursuit of antimicrobial compounds that disrupt PqsE and, in turn, quorum-sensing-directed virulence.

Finally, it is curious that the tryptophan substitution at PqsE residue 182 (PqsE E182W) that disrupts the ability of PqsE to interact with RhlR is buried deep within the PqsE active site (Figure 2c,d). This location makes it unlikely that E182 participates directly in the PqsE−RhlR protein−protein interaction interface. Rather, the finding suggests that the PqsE enzyme active site may be allosterically connected to the RhlR-interaction site. The physiological importance of this allostery remains unknown, but our discovery of this interaction opens up the possibility for follow-up investigations into the identities of substrates and products of PqsE-catalyzed hydrolysis. Specifically, the only annotated substrate for PqsE is 2-ABA-CoA. As mentioned in the Introduction, PqsE is not


https://doi.org/10.1021/acschembio.1c00049
ACS Chem. Biol. 2021, 16, 740−752

absolutely required for converting 2-ABA-CoA to 2-ABA in the PQS biosynthetic pathway. In the new context of PqsE residing in close physical proximity to RhlR, it will be particularly interesting to identify additional *in vivo* PqsE substrates. Are there small molecule products of PqsE catalysis that subsequently bind to and modulate RhlR? Alternatively, does PqsE prevent small molecules from interacting with RhlR by catalyzing their hydrolysis? Does ligand binding to either protein affect this protein−protein interaction? If so, does the identity of the bound ligand determine the strength of the PqsE−RhlR interaction? We speculate that our unveiling of the PqsE−RhlR protein−protein interaction may accelerate progress in the discovery of the physiologically relevant *in vivo* reaction catalyzed by PqsE. Identification of that biochemical pathway could answer long-standing questions about the crucial, yet currently mysterious, function that PqsE plays in *P. aeruginosa* quorum sensing.

## MATERIALS AND METHODS

**Strains, Media, and Molecular Procedures.** *P. aeruginosa* UCBPP-PA14 was used for all experiments and strain constructions (referred to here as PA14). PqsE variants were constructed using a previously reported site-directed mutagenesis protocol with *pqsE* cloned on a plasmid.[40] Primers were designed by following the Agilent Quikchange mutagenesis guidelines. Electrocompetent *P. aeruginosa* strains were transformed as described previously.[41] All strains generated in this study are listed in Table S1. Unless otherwise stated, strains were grown in Luria−Bertani broth (Fisher). Antibiotics were used as follows: ampicillin (200 μg/mL), kanamycin (100 μg/mL), tetracycline (10 μg/mL), and carbenicillin (400 μg/mL). qRT-PCR analyses of select transcripts in PA14 strains were performed as described.[17]

**Protein Expression and Purification.** 6xHis-PqsE was expressed and purified from recombinant *E. coli* as described previously[27] with modifications. Briefly, protein was purified from *E. coli* BL21(DE3) harboring a pET28b vector containing the DNA encoding 6xHis-PqsE and variants. Cultures were grown with agitation at 37 °C to $OD_{600}$ = 0.5. Protein production was induced by the addition of 1 mM IPTG followed by incubation with shaking at 37 °C for 4 h. The cells were harvested by centrifugation at 4000 rpm for 20 min and stored frozen at −80 °C. The pellet was thawed in lysis buffer (50 mM Tris-HCl, 150 mM NaCl, 20 mM imidazole, pH 8.0) supplemented with EDTA-free protease inhibitor tablets (Roche), and subsequently, the cells were lysed by sonication. The lysate was cleared by centrifugation at 12 000 rpm for 30 min, followed by incubation with Ni-NTA resin (Qiagen) for 1.5 h, before being packed into a gravity flow column. The column was washed with 10 column volumes of lysis buffer, and 6xHis-PqsE protein was eluted in elution buffer (50 mM Tris-HCl, 150 mM NaCl, 500 mM imidazole, pH 8.0). The eluate was subjected to overnight dialysis into gel filtration buffer (50 mM Tris-HCl, 150 mM NaCl, pH 8.0), prior to concentration to ∼1 mL and injection onto a Superdex 200 size-exclusion column for FPLC-assisted purification (Akta GE). Fractions containing a pure 34 kDa protein (determined by SDS-PAGE) were collected, pooled, and concentrated to ∼2 mg $mL^{-1}$ followed by storage at −80 °C. Purification of PqsE protein for use in crystallography analyses had the following modifications: during overnight dialysis, the 6xHis tag was removed by the addition of biotinylated thrombin (Millipore 69022). Prior to size-exclusion chromatography, the biotinylated thrombin was removed on streptavidin-coated resin, and a second Ni purification was performed to remove any remaining PqsE containing the 6xHis tag. Following size-exclusion chromatography, the pooled PqsE-containing fractions were concentrated to ∼10 mg $mL^{-1}$ and stored at 4 °C until use.

**High-Throughput Differential Scanning Fluorimetry Screen.** Compounds were screened for the ability to bind and shift the melting temperature ($T_m$) of purified 6xHis-PqsE using differential scanning fluorimetry (DSF). Compound solutions were prepared in DMSO and subsequently diluted in assay buffer (50 mM Tris, 150 mM NaCl, 2 mM $MnCl_2$, pH 8.0) to achieve a final screening concentration of 37 μM compound in 1.85% DMSO. Compound solutions were transferred to the wells of a 384-well PCR plate (Matrix) using a PlateMate Plus liquid handler (Matrix) and control wells were prepared with DMSO (negative control) or 100 μM C1 (positive control). Plates were subjected to centrifugation for 10 s at 1000 rpm prior to the addition of a PqsE and dye master mix in assay buffer, so that the final concentrations of PqsE and SYPRO Orange were 4 μM and 20×, respectively. Plates were sealed with transparent seals (Excel Scientific) and subjected to centrifugation for 2 min at 2000 rpm. SYPRO Orange fluorescence (ex, 470 nm; em, 623 nm) was measured in a ViiA 7 Real-Time PCR system over an increasing temperature gradient from 50 to 90 °C (temperature increased at a rate of 0.1 °C/s). For the initial high-throughput screen, $T_m$ was determined from first derivative plots of the raw fluorescence curves using custom scripts. In all subsequent experiments, $T_m$ was determined using the Prism 8.0 software. Follow-up DSF assays were performed under similar conditions, with some modifications. Briefly, PqsE proteins were tested at 5 μM, compounds were assayed at 100 μM in a final concentration of 5% DMSO, and SYPRO Orange was used at 10×. The assay buffer in follow-up assays was 50 mM Tris, 150 mM NaCl, 200 μM $MnCl_2$, and 10% glycerol, at pH 8.0, and measurements were made in a Quant Studio 6 Flex System (ThermoFisher).

**Esterase Assay Measuring MU-Butyrate Hydrolysis.** To measure PqsE enzyme activity, purified 6xHis-PqsE in assay buffer (50 mM Tricine, 0.01% Triton X-100, pH 8.5) was added to the wells of an opaque 384-well plate (Corning 3571) at 125 nM. MU-butyrate (Sigma) in assay buffer was added to the wells at a final concentration of 2 μM in a total volume of 20 μL per well. The plate was immediately incubated at RT in a Synergy plate-reader (BioTek), and fluorescence was monitored every 30 s for 30 min (ex, 360 nm; em, 450 nm). The fluorescence intensity measured after 2.5 min was plotted and normalized to the activity of WT PqsE. To assess the potencies of putative PqsE inhibitors, purified PqsE proteins were added at 200 nM to wells along with different concentrations of inhibitors supplied in DMSO, with a final DMSO concentration of 5%. Subsequently, MU-butyrate substrate was added at a final concentration of 2 μM, and the plate was incubated at RT for 20 min, prior to fluorescence quantitation. Control wells containing the inhibitor dilution series with MU-butyrate but lacking PqsE were included to establish the baseline fluorescence values, as well as to account for any inhibitor-derived fluorescence. $IC_{50}$ curves were generated using the Prism 8.0 software.

**Protein Crystallography.** Crystals were grown at 22 °C using the hanging drop vapor diffusion method with a ∼10 mg $mL^{-1}$ protein solution mixed at a 1:1 ratio with crystallization buffer (0.1 M HEPES pH 7.5, 0.2 M $MgCl_2$, 32% (w/v) PEG 400). Crystals typically formed within 48 h at 22 °C. PqsE-ligand cocrystals were formed by soaking existing PqsE crystals with compound at 70−150 μM concentration in the crystallization drop for up to 48 h. No additional cryoprotectant was required prior to flash-cooling in liquid nitrogen. Crystals grew in space group $P3_221$ with $a = b = 60.7$ Å, $c = 146.2$ Å, $\alpha = \beta = 90°$, $\gamma = 120$ °C in a crystal form previously reported for PqsE with a single protomer in the asymmetric unit.[25] Data were collected from flash-cooled crystals maintained at 100 K at the AMX (17-ID-1) beamline of the National Synchrotron Light Source II, processed with XDS[42] and merged with AIMLESS.[43] The starting model for the structure was from PDB entry 2Q0I.[25] The structure was iteratively rebuilt with Coot[44] and refined with PHENIX[45] with ligands built into unambiguous differences in density in the active site. Ligands were refined with partial occupancy (0.81 for BB391 and 0.82 for BB393) with a TLS B-factor model for the protein atoms. Final refinement statistics are shown in the Supporting Information. The final structures were deposited in the Protein Data Bank with identifiers 7KGW (PqsE-BB391) and 7KGX (PqsE-BB393).

**Fluorescence Polarization Compound Binding and Competition Assays.** Dilutions of purified 6xHis-PqsE proteins were prepared in assay buffer (50 mM Tricine, 2 μM $MnCl_2$, 0.01% Triton


https://doi.org/10.1021/acschembio.1c00049
ACS Chem. Biol. 2021, 16, 740−752

X-100, pH 8.5) and added to the wells of an opaque 384-well plate (Corning 3571) at a final volume of 20 μL per well. BB562 was diluted in assay buffer and added to the wells at a final concentration of 250 nM, and the plate was incubated at RT for 30 min. Fluorescence polarization was measured in a Synergy Neo2 plate-reader (Biotek) with excitation and emission wavelengths of 485 and 530 nm, respectively. $K_{app}$ values were determined using the Prism 8.0 software. For competition assays, 6xHis-PqsE was diluted to a final concentration of 250 nM in assay buffer and added to wells. The specified concentrations of competitor molecules in DMSO were added to the wells such that the final DMSO concentration was 5%. The protein−inhibitor complexes were allowed to form at RT for 10 min, followed by the addition of BB562 at a final concentration of 250 nM. The plate was incubated at RT for 30 min prior to the measurement of fluorescence polarization. $EC_{50}$ values were determined using a variable slope inhibition curve fit to the data in the Prism 8.0 software.

**Pyocyanin Assay.** Overnight cultures of the Δ*pqsE P. aeruginosa* strain carrying the pUCP18 vector or the vector harboring WT or mutant *pqsE* genes were grown from single colonies in LB medium supplemented with carbenicillin at 37 °C. The cultures were diluted 1:1000 in 2 mL of fresh LB liquid medium with antibiotics and grown with shaking at 37 °C for 17 h. One milliliter of each culture was subjected to centrifugation at 13 000 rpm for 3 min. The clarified supernatants were collected, and the $OD_{695}$ measured in a Beckman Coulter DU730 Spectrophotometer. The pellets were resuspended in PBS, and $OD_{600}$ was measured to determine the cell density of each sample. Pyocyanin production was determined by normalizing $OD_{695}$ of the clarified supernatant to the $OD_{600}$ of the resuspended pellet. When added, test compounds were supplied at 100 μM in DMSO (final DMSO concentration = 1%) prior to the 17 h shaking incubation.

**PqsE−RhlR Coupled P*rhlA-lux* Assay.** Overnight cultures of *E. coli* strains harboring plasmids with *rhlR* driven by the $P_{BAD}$ promoter, *luxCDABE* under the P*rhlA* promoter, and either the pACYC184 vector or pACYC184 harboring WT *pqsE* or mutant *pqsE* alleles were grown from single colonies at 37 °C in LB medium supplemented with ampicillin, kanamycin, and tetracycline. The overnight cultures were diluted 1:100 into fresh LB medium containing antibiotics and 0.1% arabinose and added to the wells of a black, clear-bottomed 96-well plate at 150 μL per well. C4-HSL was added to the wells at 200 nM (1% DMSO). Plates were incubated for 8 h at 37 °C with shaking. Subsequently, bioluminescence and $OD_{600}$ were measured in an Envision 2104 plate reader. Bioluminescence values are reported normalized to cell density ($OD_{600}$).

**PqsE−RhlR Interaction Pull-Down Assay.** RhlR was produced using a previously reported method.[32] Briefly, 25 mL cultures of *E. coli* BL21 (DE3) carrying *rhlR* on pET23b were grown to $OD_{600}$ = 0.5, and expression of *rhlR* was induced by the addition of 1 mM IPTG, simultaneous with the addition of 100 μM mBTL. After 4 h at 25 °C, cells were collected by centrifugation, and pellets were frozen. For use, frozen pellets were resuspended in lysis buffer (50 mM Tris-HCl, 150 mM NaCl, 20 mM imidazole, pH 8.0) and lysed by sonication. Lysates were cleared by centrifugation at 13 000 rpm for 30 min, and the soluble fraction was collected. Lysates (100 μL) were combined with purified 6xHis-PqsE proteins at a final concentration of 9 μM 6xHis-PqsE in 200 μL total volume. The mixtures were allowed to incubate at 4 °C for 30 min prior to the addition of a 10 μL settle volume of MagneHis Ni Resin (Promega). Incubation was continued for an additional 1 h at 4 °C with turning. After incubation, aliquots of the lysate/PqsE/bead mixture were collected as "input" samples and prepared for SDS-PAGE analysis. The remaining mixtures were pelleted using a magnetic stand, and the resin was washed three times with lysis buffer. Ni-bound 6xHis-PqsE complexes were eluted in 200 μL elution buffer (50 mM Tris-HCl, 150 mM NaCl, 500 mM imidazole, pH 8.0), and prepared for SDS-PAGE analysis. Input and elution samples were subjected to SDS-PAGE on stain-free gels (Bio-Rad) and subsequently imaged after UV activation of the in-gel protein stain.

## ■ ASSOCIATED CONTENT

### Supporting Information

The Supporting Information is available free of charge at https://pubs.acs.org/doi/10.1021/acschembio.1c00049.

One table, eight figures, extended screening methods, crystallography and refinement statistics, and synthetic methods (PDF)

## ■ AUTHOR INFORMATION


### Corresponding Author

**Bonnie L. Bassler** − *Department of Molecular Biology, Princeton University, Princeton, New Jersey 08544, United States; Howard Hughes Medical Institute, Chevy Chase, Maryland 20815, United States;* orcid.org/0000-0002-0043-746X; Email: bbassler@princeton.edu

### Authors

**Isabelle R. Taylor** − *Department of Molecular Biology, Princeton University, Princeton, New Jersey 08544, United States;* orcid.org/0000-0003-1053-5677

**Jon E. Paczkowski** − *Department of Health, Wadsworth Center, Albany, New York 12208, United States; Department of Biomedical Sciences, University at Albany School of Public Health, Albany, New York 12201, United States*

**Philip D. Jeffrey** − *Department of Molecular Biology, Princeton University, Princeton, New Jersey 08544, United States*

**Brad R. Henke** − *Opti-Mol Consulting, LLC, Cary, North Carolina 27518, United States*

**Chari D. Smith** − *Department of Molecular Biology, Princeton University, Princeton, New Jersey 08544, United States*

Complete contact information is available at: https://pubs.acs.org/10.1021/acschembio.1c00049


### Notes

The authors declare no competing financial interest.

## ■ ACKNOWLEDGMENTS

We thank members of the Bassler laboratory for helpful advice and discussions, especially G. Whitney for performing the qRT-PCR experiments. The high-throughput DSF screen and initial enzyme assays with potential hit molecules were performed at Bienta. Molecules used in this study were synthesized at WuXi AppTec. Protein crystallography was performed in the Macromolecular Crystallography Core Facility at Princeton University. The AMX beamline of the National Synchrotron Light Source II, a U.S. Department of Energy (DOE) Office of Science User Facility operated for the DOE Office of Science by Brookhaven National Laboratory was also used under Contract DE-SC0012704. This work was supported by the Howard Hughes Medical Institute, NIH grant 2R37GM065859, and National Science Foundation grant MCB-1713731 to B. Bassler, NIH grant F32GM134583 to I. Taylor, and New York Community Trust Foundation grant P19-000454 to J. Paczkowski. The content herein is solely the responsibility of the authors and does not represent the official views of the National Institutes of Health.

## ■ REFERENCES

(1) Driscoll, J. A., Brody, S. L., and Kollef, M. H. (2007) The epidemiology, pathogenesis and treatment of *Pseudomonas aeruginosa* infections. *Drugs 67*, 351−368.

(2) Smith, E. E., Buckley, D. G., Wu, Z., Saenphimmachak, C., Hoffman, L. R., D'Argenio, D. A., Miller, S. I., Ramsey, B. W., Speert, D. P., Moskowitz, S. M., Burns, J. L., Kaul, R., and Olson, M. V. (2006) Genetic adaptation by *Pseudomonas aeruginosa* to the airways of cystic fibrosis patients. *Proc. Natl. Acad. Sci. U. S. A. 103*, 8487−8492.
(3) Holder, I. A. (1993) *P. aeruginosa* Burn Infections: Pathogenesis and Treatment, in *Pseudomonas aeruginosa as an Opportunistic Pathogen*, pp 275−295, Springer, Boston, MA.
(4) Maurice, N. M., Bedi, B., and Sadikot, R. T. (2018) *Pseudomonas aeruginosa* Biofilms: Host Response and Clinical Implications in Lung Infections. *Am. J. Respir. Cell Mol. Biol. 58*, 428−439.
(5) Tan, M.-W., Rahme, L. G., Sternberg, J. A., Tompkins, R. G., and Ausubel, F. M. (1999) *Pseudomonas aeruginosa* killing of *Caenorhabditis elegans* used to identify *P. aeruginosa* virulence factors. *Proc. Natl. Acad. Sci. U. S. A. 96*, 2408.
(6) Pang, Z., Raudonis, R., Glick, B. R., Lin, T.-J., and Cheng, Z. (2019) Antibiotic resistance in *Pseudomonas aeruginosa*: mechanisms and alternative therapeutic strategies. *Biotechnol. Adv. 37*, 177−192.
(7) Boucher, H. W., Talbot, G. H., Bradley, J. S., Edwards, J. E., Gilbert, D., Rice, L. B., Scheld, M., Spellberg, B., and Bartlett, J. (2009) Bad bugs, no drugs: no ESKAPE! An update from the Infectious Diseases Society of America. *Clin. Infect. Dis. 48*, 1−12.
(8) Osmon, S., Ward, S., Fraser, V. J., and Kollef, M. H. (2004) Hospital mortality for patients with bacteremia due to *Staphylococcus aureus* or *Pseudomonas aeruginosa*. *Chest 125*, 607−616.
(9) Miller, M. B., and Bassler, B. L. (2001) Quorum sensing in bacteria. *Annu. Rev. Microbiol. 55*, 165−199.
(10) Pearson, J. P., Passador, L., Iglewski, B. H., and Greenberg, E. P. (1995) A second N-acylhomoserine lactone signal produced by *Pseudomonas aeruginosa*. *Proc. Natl. Acad. Sci. U. S. A. 92*, 1490−1494.
(11) Whiteley, M., Lee, K. M., and Greenberg, E. P. (1999) Identification of genes controlled by quorum sensing in *Pseudomonas aeruginosa*. *Proc. Natl. Acad. Sci. U. S. A. 96*, 13904−13909.
(12) Pesci, E. C., Pearson, J. P., Seed, P. C., and Iglewski, B. H. (1997) Regulation of las and rhl quorum sensing in *Pseudomonas aeruginosa*. *J. Bacteriol. 179*, 3127−3132.
(13) Heeb, S., Fletcher, M. P., Chhabra, S. R., Diggle, S. P., Williams, P., and Cámara, M. (2011) Quinolones: from antibiotics to autoinducers. *FEMS Microbiology Reviews 35*, 247−274.
(14) Lau, G. W., Hassett, D. J., Ran, H., and Kong, F. (2004) The role of pyocyanin in *Pseudomonas aeruginosa* infection. *Trends Mol. Med. 10*, 599−606.
(15) Choi, W., Choe, S., Lin, J., Borchers, M. T., Kosmider, B., Vassallo, R., Limper, A. H., and Lau, G. W. (2020) Exendin-4 restores airway mucus homeostasis through the GLP1R-PKA-PPARγ-FOXA2-phosphatase signaling. *Mucosal Immunol. 13*, 637−651.
(16) Drees, S. L., and Fetzner, S. (2015) PqsE of *Pseudomonas aeruginosa* Acts as Pathway-Specific Thioesterase in the Biosynthesis of Alkylquinolone Signaling Molecules. *Chem. Biol. 22*, 611−618.
(17) Mukherjee, S., Moustafa, D. A., Stergioula, V., Smith, C. D., Goldberg, J. B., and Bassler, B. L. (2018) The PqsE and RhlR proteins are an autoinducer synthase-receptor pair that control virulence and biofilm development in *Pseudomonas aeruginosa*. *Proc. Natl. Acad. Sci. U. S. A. 115*, E9411−E9418.
(18) Farrow, J. M., Sund, Z. M., Ellison, M. L., Wade, D. S., Coleman, J. P., and Pesci, E. C. (2008) PqsE functions independently of PqsR-Pseudomonas quinolone signal and enhances the rhl quorum-sensing system. *J. Bacteriol. 190*, 7043−7051.
(19) Groleau, M.-C., de Oliveira Pereira, T., Dekimpe, V., and Déziel, E. (2020) PqsE Is Essential for RhlR-Dependent Quorum Sensing Regulation in *Pseudomonas aeruginosa*. *mSystems 5*, e00194-20.
(20) Mukherjee, S., Moustafa, D., Smith, C. D., Goldberg, J. B., and Bassler, B. L. (2017) The RhlR quorum-sensing receptor controls *Pseudomonas aeruginosa* pathogenesis and biofilm development independently of its canonical homoserine lactone autoinducer. *PLoS Pathog. 13*, No. e1006504.
(21) O'Loughlin, C. T., Miller, L. C., Siryaporn, A., Drescher, K., Semmelhack, M. F., and Bassler, B. L. (2013) A quorum-sensing inhibitor blocks *Pseudomonas aeruginosa* virulence and biofilm formation. *Proc. Natl. Acad. Sci. U. S. A. 110*, 17981−17986.
(22) Boursier, M. E., Moore, J. D., Heitman, K. M., Shepardson-Fungairino, S. P., Combs, J. B., Koenig, L. C., Shin, D., Brown, E. C., Nagarajan, R., and Blackwell, H. E. (2018) Structure-Function Analyses of the N-Butanoyl l-Homoserine Lactone Quorum-Sensing Signal Define Features Critical to Activity in RhlR. *ACS Chem. Biol. 13*, 2655−2662.
(23) Zender, M., Witzgall, F., Drees, S. L., Weidel, E., Maurer, C. K., Fetzner, S., Blankenfeldt, W., Empting, M., and Hartmann, R. W. (2016) Dissecting the Multiple Roles of PqsE in *Pseudomonas aeruginosa* Virulence by Discovery of Small Tool Compounds. *ACS Chem. Biol. 11*, 1755−1763.
(24) Baldelli, V., D'Angelo, F., Pavoncello, V., Fiscarelli, E. V., Visca, P., Rampioni, G., and Leoni, L. (2020) Identification of FDA-approved antivirulence drugs targeting the *Pseudomonas aeruginosa* quorum sensing effector protein PqsE. *Virulence 11*, 652−668.
(25) Yu, S., Jensen, V., Seeliger, J., Feldmann, I., Weber, S., Schleicher, E., Häussler, S., and Blankenfeldt, W. (2009) Structure elucidation and preliminary assessment of hydrolase activity of PqsE, the Pseudomonas quinolone signal (PQS) response protein. *Biochemistry 48*, 10298−10307.
(26) Folch, B., Déziel, E., and Doucet, N. (2013) Systematic Mutational Analysis of the Putative Hydrolase PqsE: Toward a Deeper Molecular Understanding of Virulence Acquisition in *Pseudomonas aeruginosa*. *PLoS One 8*, No. e73727.
(27) Valastyan, J. S., Tota, M. R., Taylor, I. R., Stergioula, V., Hone, G. A. B., Smith, C. D., Henke, B. R., Carson, K. G., and Bassler, B. L. (2020) Discovery of PqsE Thioesterase Inhibitors for *Pseudomonas aeruginosa* Using DNA-Encoded Small Molecule Library Screening. *ACS Chem. Biol. 15*, 446−456.
(28) Vaneechoutte, M., Verschraegen, G., Claeys, G., and Flamen, P. (1988) Rapid identification of *Branhamella catarrhalis* with 4-methylumbelliferyl butyrate. *J. Clin. Microbiol. 26*, 1227−1228.
(29) Kübler, D., Ingenbosch, K. N., Bergmann, A., Weidmann, M., and Hoffmann-Jacobsen, K. (2015) Fluorescence spectroscopic analysis of the structure and dynamics of *Bacillus subtilis* lipase A governing its activity profile under alkaline conditions. *Eur. Biophys. J. 44*, 655−665.
(30) Page, M. I., and Badarau, A. (2008) The mechanisms of catalysis by metallo beta-lactamases. *Bioinorg. Chem. Appl. 2008*, 576297.
(31) Rampioni, G., Falcone, M., Heeb, S., Frangipani, E., Fletcher, M. P., Dubern, J.-F., Visca, P., Leoni, L., Cámara, M., and Williams, P. (2016) Unravelling the Genome-Wide Contributions of Specific 2-Alkyl-4-Quinolones and PqsE to Quorum Sensing in *Pseudomonas aeruginosa*. *PLoS Pathog. 12*, No. e1006029.
(32) McCready, A. R., Paczkowski, J. E., Cong, J.-P., and Bassler, B. L. (2019) An autoinducer-independent RhlR quorum-sensing receptor enables analysis of RhlR regulation. *PLoS Pathog. 15*, No. e1007820.
(33) Lister, P. D., Wolter, D. J., and Hanson, N. D. (2009) Antibacterial-resistant *Pseudomonas aeruginosa*: clinical impact and complex regulation of chromosomally encoded resistance mechanisms. *Clin. Microbiol. Rev. 22*, 582−610.
(34) Sharp, L. L., Zhou, J., and Blair, D. F. (1995) Features of MotA proton channel structure revealed by tryptophan-scanning mutagenesis. *Proc. Natl. Acad. Sci. U. S. A. 92*, 7946−7950.
(35) Rasmussen, T., Rasmussen, A., Singh, S., Galbiati, H., Edwards, M. D., Miller, S., and Booth, I. R. (2015) Properties of the Mechanosensitive Channel MscS Pore Revealed by Tryptophan Scanning Mutagenesis. *Biochemistry 54*, 4519−4530.
(36) Vallée-Bélisle, A., and Michnick, S. W. (2012) Visualizing transient protein-folding intermediates by tryptophan-scanning mutagenesis. *Nat. Struct. Mol. Biol. 19*, 731−736.
(37) Tang, Q., Villar, M. T., Artigues, A., Thyfault, J. P., Apte, U., Zhu, H., Peterson, K. R., and Fenton, A. W. (2019) Mutational

mimics of allosteric effectors: a genome editing design to validate allosteric drug targets. *Sci. Rep. 9*, 9031.
(38) Hancock, R. E. (1998) Resistance mechanisms in *Pseudomonas aeruginosa* and other nonfermentative gram-negative bacteria. *Clin. Infect. Dis. 27*, S93−S99.
(39) Breidenstein, E. B. M., de la Fuente-Núñez, C., and Hancock, R. E. W. (2011) *Pseudomonas aeruginosa*: all roads lead to resistance. *Trends Microbiol. 19*, 419−426.
(40) McCready, A. R., Paczkowski, J. E., Henke, B. R., and Bassler, B. L. (2019) Structural determinants driving homoserine lactone ligand selection in the *Pseudomonas aeruginosa* LasR quorum-sensing receptor. *Proc. Natl. Acad. Sci. U. S. A. 116*, 245.
(41) Choi, K.-H., Kumar, A., and Schweizer, H. P. (2006) A 10-min method for preparation of highly electrocompetent *Pseudomonas aeruginosa* cells: Application for DNA fragment transfer between chromosomes and plasmid transformation. *J. Microbiol. Methods 64*, 391−397.
(42) Kabsch, W. (2010) XDS. *Acta Crystallogr., Sect. D: Biol. Crystallogr. 66*, 125−132.
(43) Evans, P. R., and Murshudov, G. N. (2013) How good are my data and what is the resolution? *Acta Crystallogr., Sect. D: Biol. Crystallogr. 69*, 1204−1214.
(44) Emsley, P., Lohkamp, B., Scott, W. G., and Cowtan, K. (2010) Features and development of Coot. *Acta Crystallogr., Sect. D: Biol. Crystallogr. 66*, 486−501.
(45) Liebschner, D., Afonine, P. V., Baker, M. L., Bunkóczi, G., Chen, V. B., Croll, T. I., Hintze, B., Hung, L. W., Jain, S., McCoy, A. J., Moriarty, N. W., Oeffner, R. D., Poon, B. K., Prisant, M. G., Read, R. J., Richardson, J. S., Richardson, D. C., Sammito, M. D., Sobolev, O. V., Stockwell, D. H., Terwilliger, T. C., Urzhumtsev, A. G., Videau, L. L., Williams, C. J., and Adams, P. D. (2019) Macromolecular structure determination using X-rays, neutrons and electrons: recent developments in Phenix. *Acta Crystallogr. D Struct Biol. 75*, 861−877.


https://doi.org/10.1021/acschembio.1c00049
*ACS Chem. Biol.* 2021, 16, 740−752